

1 Characterising tandem repeat complexities across

2 long-read sequencing platforms with TREAT and

3 *otter*

4

5 Niccolo' Tesi,^{1,2,3,*,#} Alex Salazar,^{1,*,#} Yaran Zhang,¹ Sven van der Lee,^{1,2}
6 Marc Hulsman,^{1,2,3} Lydian Knoop,¹ Sanduni Wijesekera,¹ Jana Krizova,¹
7 Anne-Fleur Schneider,¹ Maartje Pennings,⁵ Kristel Sleegers,⁴ Erik-Jan
8 Kamsteeg,⁵ Marcel Reinders,³ & Henne Holstege ^{1,2,3,#}

9 * Authors contributed equally

10 # Corresponding authors

11

12 ¹ Section Genomics of Neurodegenerative Diseases and Aging, Department of Clinical Genetics, Vrije
13 Universiteit Amsterdam, Amsterdam UMC, Amsterdam, The Netherlands

14 ² Alzheimer Center Amsterdam, Department of Neurology, Amsterdam Neuroscience, Vrije Universiteit
15 Amsterdam, Amsterdam UMC, Amsterdam, The Netherlands

16 ³ Delft Bioinformatics Lab, Delft University of Technology, Delft, The Netherlands

17 ⁴ Complex Genetics of Alzheimer's Disease Group, Antwerp Center for Molecular Neurology, VIB,
18 Antwerp B-2610, Belgium

19 ⁵ Department of Genome Diagnostics, Radboud University Medical Center, Nijmegen, The Netherlands

20

21 *Keywords*

22 LRS Special Issue; Tandem repeats; Long-read sequencing; PacBio; Nanopore; Genotyping;
23 Cross-platform compatibility;

24

25

26 Abstract

27 Tandem repeats (TR) play important roles in genomic variation and disease risk in humans.
28 Long-read sequencing allows for the accurate characterisation of TRs, however, the
29 underlying bioinformatics perspectives remain challenging.
30 We present *otter* and TREAT: *otter* is a fast targeted local assembler, cross-compatible across
31 different sequencing platforms. It is integrated in TREAT, an end-to-end workflow for TR
32 characterisation, visualisation and analysis across multiple genomes.
33 In a comparison with existing tools based on long-read sequencing data from both Oxford
34 Nanopore Technology (ONT, Simplex and Duplex) and PacBio (Sequel 2 and Revio), *otter*
35 and TREAT achieved state-of-the-art genotyping and motif characterisation accuracy.
36 Applied to clinically relevant TRs, TREAT/*otter* significantly identified individuals with
37 pathogenic TR expansions. When applied to a case-control setting, we significantly replicated
38 previously reported associations of TRs with Alzheimer's Disease, including those near or
39 within *APOC1* ($p=2.63\times 10^{-9}$), *SPI1* ($p=6.5\times 10^{-3}$) and *ABCA7* ($p=0.04$) genes.
40 We finally used TREAT/*otter* to systematically evaluate potential biases when genotyping TRs
41 using diverse ONT and PacBio long-read sequencing datasets. We showed that, in rare cases
42 (0.06%), long-read sequencing suffers from coverage drops in TRs, including the disease-
43 associated TRs in *ABCA7* and *RFC1* genes. Such coverage drops can lead to TR mis-
44 genotyping, hampering the accurate characterisation of TR alleles.
45 Taken together, our tools can accurately genotype TR across different sequencing
46 technologies and with minimal requirements, allowing end-to-end analysis and comparisons
47 of TR in human genomes, with broad applications in research and clinical fields.

48

49 1. Introduction

50 Roughly 30% of the human genome consists of tandem repeats (TR) characterised by one or
51 more repeat motifs that are defined by their consecutive repetition.¹ This repetitive pattern
52 often leads to DNA instability, facilitating not only expansions and contractions of the repeating
53 motif sequence, but also allelic diversity within the sequence.^{2,3} Several definitions of TRs
54 have been introduced based on the motif length and size variability, including microsatellites,
55 minisatellites, and macrosatellites. Microsatellites (or short tandem repeats, STR) are the most
56 abundant TRs in the human genome, are characterised by a repetitive motif of less than 6
57 base pairs (bp), and tend to cluster in non-coding regions of the genome.⁴ Minisatellites are
58 characterised by a repetitive motif with a size ranging 7-100 bp, and they are highly enriched
59 in the telomeric regions of the genome.⁵ Macrosatellites are characterised by larger tandem
60 repeat units (>100 bp), and are enriched in the telomeric and centromeric portions of the
61 genome.⁶

62

63 TRs can disrupt gene-expression regulation and contribute to over 40 neurological
64 disorders.^{1,7,8} Pathogenic TR expansions, surpassing critical lengths, are linked to conditions
65 like spinocerebellar ataxias, Huntington's disease, Fragile-X syndrome, Amyotrophic lateral
66 sclerosis (ALS), and Myotonic Dystrophy.⁷⁻⁹ For instance, Fragile-X syndrome results from a
67 GGC repeat expansion in the *FMR1* gene, with affected individuals having up to 4,000 copies
68 compared to less than 50 in healthy individuals.¹⁰ Similarly, ALS is caused by an intronic hexa-
69 nucleotide repeat expansion (GCCCGG) in the *C9orf72* gene, exceeding a critical length of
70 more than 200 copies.¹¹ Beyond diseases-causing, TRs have been also identified as risk
71 factor for complex human diseases: for example, the intronic TR in the *ABCA7* gene is
72 associated with a 4.5-fold increased risk of Alzheimer's Disease (AD) when the TR exceeds
73 5720 base pairs.^{12,13}

74

75 Traditionally, the evaluation of TR lengths and sequences has been challenging. Conventional
76 methods, such as repeat-primed polymerase chain reaction (RP-PCR) and Southern blot
77 assays, are time-consuming and limited in detecting TRs within PCR-based boundaries.
78 Short-read sequencing approaches offer an alternative, but their limited read lengths often fail
79 to span repetitive regions effectively. Despite heuristic methods and statistical modelling,^{14–19}
80 accurately assessing clinically relevant TRs remains difficult. The advent of long-read
81 sequencing, particularly with PacBio's High Fidelity (HiFi) and Oxford Nanopore Technology's
82 (ONT) Duplex technology (10–20kb on average, >99% accuracy),^{20,21} has significantly
83 improved TR evaluation by providing long and accurate sequencing fragments.

84

85 Characterising TRs with long-read sequencing technology currently has two main limitations.
86 First, there is the need to characterise TRs across different (long-read) sequencing
87 technologies and data-types.^{22–24} This is critically important given the growing long-read
88 sequencing initiatives aiming to comprehensively assess TRs in large genomic datasets,²⁵
89 spanning both population-wide and clinical contexts. For example, some existing tools are
90 constrained by predefined TR databases, hindering the identification of new TR features such
91 as novel motif sequences;²⁶ other tools are technology and data-type-dependent,²² or do not
92 produce generalizable multi-sample outputs.^{23,24}

93

94 Second, there is a lack of comprehensive studies that have investigated potential biases when
95 sequencing TRs. For example, DNA methylation has been previously shown to impact base-
96 calling accuracy in long-read sequencing data.^{27–29} Similarly, the formation of secondary
97 structures due to TRs could impact enzyme efficiency (e.g. polymerase or nanopores),³⁰
98 potentially reducing read-quality and sequencing throughput in current long-read sequencing
99 technologies. Furthermore, some technologies require the alignment of noisy reads to
100 generate high quality consensus sequences, which might be more difficult in case of repetitive

101 regions. These problems may impact genotyping accuracy and lead to incorrect assessments
102 of allele-sequences, including disease-associated TRs in patients.

103

104 Here, we present TREAT (Tandem REpeat Annotation Toolkit), a unified workflow for
105 characterising TRs across multiple genomes, cross-compatible with diverse long-read
106 technologies and data-types (e.g. read-alignments and *de novo* assemblies). TREAT employs
107 a novel generic targeted local assembler, *otter*, that can adapt to different sequencing
108 chemistries to accurately characterise TRs. We benchmarked TREAT and *otter* with currently
109 available tools for TR genotyping (PacBio's TRGT and LongTR)^{22,31} in terms of genotyping
110 accuracy, motif identification, and running performances. We then showcase TREAT and *otter*
111 applicability in a population-, clinical-, and case-control setting. Finally, we performed a
112 systematic analysis of ~864K genome-wide TRs in CHM13 reference genome to evaluate
113 sporadic coverage drops that can affect TR genotyping accuracy. We did so using the well-
114 characterised HG002 genome based on long-read sequencing data from ONT (Duplex and
115 Simplex), HiFi and non-HiFi data from PacBio's Revio and Sequel 2 instruments.

116

117 **2. Results**

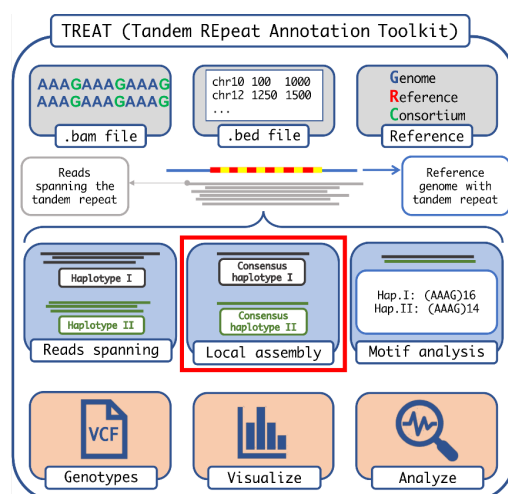
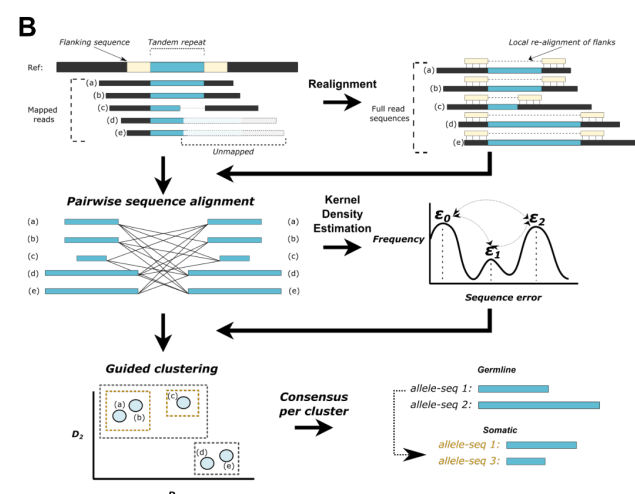
118 **2.1 Cross-compatible workflow for characterising tandem** 119 **repeats with *otter* and TREAT**

120 We present *otter* and TREAT, two bioinformatic tools that enable tandem repeat (TR)
121 characterisation across different long-read sequencing technologies and data-types with
122 minimal input requirements (*Figure 1*). *Otter* is a stand-alone generic targeted local assembler
123 for long-read sequencing data, which automatically adapts to sequencing error-rates and
124 coverage levels per target region. TREAT integrates *otter* to enable end-to-end unified
125 workflow for *de novo* motif characterisation and downstream analysis, including TR

126 visualisation, outlier-based and case-control comparisons (see *Methods*). Both tools require
127 sequencing data aligned to a reference genome (.bam files), the reference genome used
128 (.fasta file), and the coordinates of the regions of interest (chromosome, start and end
129 positions encoded in a .bed file). TREAT/otter outputs a multi-sample gVCF (Genomic Variant
130 Call Format) file reporting genotyped alleles, their size and relative repeat content (motif and
131 number of copies), of each TR in each sample.

132
133 Otter is written in C++ and the source code is freely available at
134 <https://github.com/holstegelab/otter>.

135
136 TREAT is written in Python and R (for plots). The source code is freely available at
137 <https://github.com/holstegelab/treat> along with example datasets, documentation, a dedicated
138 Conda configuration file and a Docker image to ease the installation.

139
A 
B 

140
141 *Figure 1: Schematic workflow of TREAT and otter.* **A.** Shows TREAT workflow, highlighting the required
142 inputs, the main features, and the main outputs of the tool. The red box highlights the main genotyping
143 engine based on *otter*. **B.** Summarises the main algorithmic steps of *otter*, a novel targeted local
144 assembler for long-read sequencing data.

145

146 2.2 *Otter* and TREAT enable accurate characterisation of both 147 PacBio and ONT long-read data

148 We benchmarked TREAT and *otter* with TRGT and LongTR,^{22,31} currently available tools to
149 characterise TRs in long-read sequencing data. We compared: (i) genotyping accuracy, *i.e.*
150 the accuracy of the predicted allele sequences for a TR, (ii) motif characterisation accuracy,
151 and (iii) computational resources. We varied different long-read sequencing technologies
152 (PacBio Sequel 2 and Revio, ONT Simplex and Duplex) as well as different coverages (5x,
153 10x, 15x, 20x, 25x, and 30x) of HG002.³² We focussed on a set of 161,382 TRs from PacBio's
154 repeat catalogue (see *Methods*). Predicted TR alleles were compared to the *expected* alleles
155 based on the HG002 T2T assembly (see *Methods*).

156

157 In PacBio data, we found comparable genotyping accuracy between *otter* (TREAT genotyping
158 engine) and TRGT, for both Sequel 2 and Revio datasets, although *otter* generated more
159 accurate genotypes for larger TRs (*e.g.* >500bp), achieving average error-rates of 0.2-2.5%,
160 compared to 0.6-3.8% of TRGT. Both methods were more accurate when increasing the
161 coverage, although this was less pronounced for larger TRs (>500 bp). Notably, genotyping
162 accuracy for both *otter* and TRGT was higher for PacBio's Sequel 2 data in comparison with
163 Revio data (*Figure 2A* and *Supplementary Results*). In ONT data, *otter* was generally more
164 accurate than LongTR although differences for large TRs were less clear. For both tools, we
165 observed better accuracies for Duplex data in comparison to Simplex data (*Figure 2B* and
166 *Supplementary Results*). Altogether, our benchmark across all tools revealed that PacBio led
167 to more accurate genotypes for TRs <500 bp, with PacBio and ONT having similar
168 performances for TRs ranging 500-1000 bp, and ONT leading to more accurate genotypes for
169 TRs >=1000 bp (see *Figure 2A-B* and *Supplementary Results*).

170

171 The above observations remain when using different distance metrics and partitioned by
172 different TR-types. For example, we observed similar performances when using the raw edit
173 distance and correlation between observed and expected allele sizes (*Figure S1* and
174 *Supplementary Results*). Furthermore, we found that TRs characterised by dinucleotide
175 repeat motifs were on average less accurate than TRs with longer motifs (*Figure S2*). The
176 fraction of alleles perfectly genotyped (*i.e.* with an edit distance of 0), compared to expected
177 alleles, increased with higher coverage across all technologies and tools (*Figure S3*), with
178 Sequel 2 data having the largest fraction of alleles perfectly matched, and ONT Simplex having
179 the least. In PacBio Sequel 2 and Revio data, TRGT generated a slightly higher fraction of
180 perfectly matched alleles with respect to *otter* (max difference 2.8%). In ONT data, *otter*
181 outperformed LongTR in all settings.

182
183 Similarly, TREAT, which makes use of TR-genotypes from *otter*, achieved similar motif
184 characterisation accuracy relative to TRGT (*Figure 2C*). In the GRCh38 reference genome,
185 the motifs of the 161K TRs were mostly dinucleotide (49%), followed by tetranucleotide (22%)
186 and 16+ bp motifs (11%) (*Figure S4*). Because LongTR does not directly report the identified
187 TR motifs, we compared TR motifs between TREAT and TRGT. On average, TREAT identified
188 the same motifs as TRGT in 96% of cases (*Figure 2C*), and this did not change for different
189 technologies (Sequel 2 or Revio) or different coverages. We observed a higher concordance
190 in motif detection between tools for shorter motifs (*Figure 2C*). When looking at the motifs
191 identified by TREAT on the GRCh38 reference genome, these matched known TR annotations
192 in 91% of the cases.

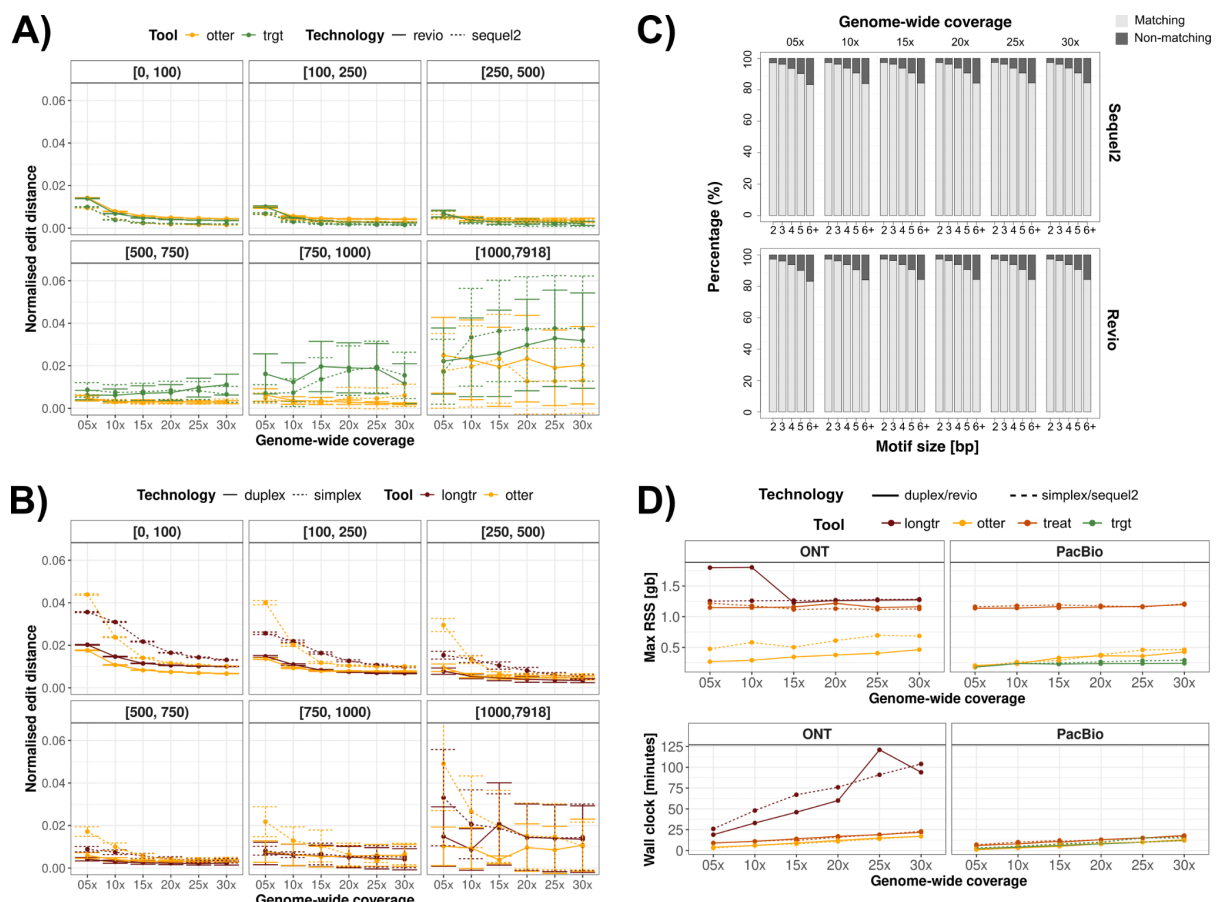
193
194 Finally, we evaluated the computational performances of *otter* (stand-alone), TREAT
195 (integrated workflow with *otter*), TRGT and LongTR. When using four threads, TRGT and *otter*
196 had similar run-time performances, while both were slightly faster than the integrated workflow
197 from TREAT (*Figure 2D*). On the other hand, for the ONT data, *otter* and TREAT were faster

198 than LongTR. In terms of memory consumption, performances were comparable between
199 TREAT and LongTR, while *otter* and TRGT used significantly less memory (*Figure 2D*). When
200 evaluating the multithreading capabilities in TREAT, we saw that when increasing the number
201 of threads to 6, 8, 10 and 12, the running times decreased by 1.3-, 1.5-, 1.6- and 1.8-fold (on
202 average across the different technologies), compared to 4 CPU threads (*Figure S5*).

203

204 In addition to the high-quality HiFi data, PacBio can output non-HiFi data, *i.e.* reads that did
205 not pass PacBio's internal HiFi quality thresholds, and that constitute a significant fraction of
206 all sequenced data (45% in HG002). We explored whether integrating both HiFi and non-HiFi
207 data could improve *otter*'s capability to accurately characterise TR allele sequences. Because
208 Revio uses a subset of these non-HiFi reads (those with at least 90% read quality) to improve
209 throughput and accuracy via DeepConsensus,³³ we performed this analysis only for Sequel 2
210 data. We found that non-HiFi data improved accuracy across all TR-lengths. Specifically, when
211 integrating non-HiFi reads of at least 85-90% read quality, genotyping accuracy improved by
212 nearly two-fold (*Figure S6*).

213



214

215 *Figure 2: Benchmarking between TREAT/otter, TRGT, and LongTR. A. Genotyping accuracy of otter*
 216 *and TRGT on PacBio Sequel 2 and Revio data, stratified by TR size and sequencing depth. B.*
 217 *Genotyping accuracy of otter and LongTR on ONT Simplex and Duplex data, stratified by TR size and*
 218 *sequencing depth. C. Motif identification accuracy of TREAT and TRGT on PacBio Sequel 2 and Revio*
 219 *data, showing the overlap of matching motifs, stratified by motif size and sequencing depth. D. Memory*
 220 *usage and running time of otter, TREAT, TRGT, and LongTR, across technologies and sequencing*
 221 *coverages.*

222

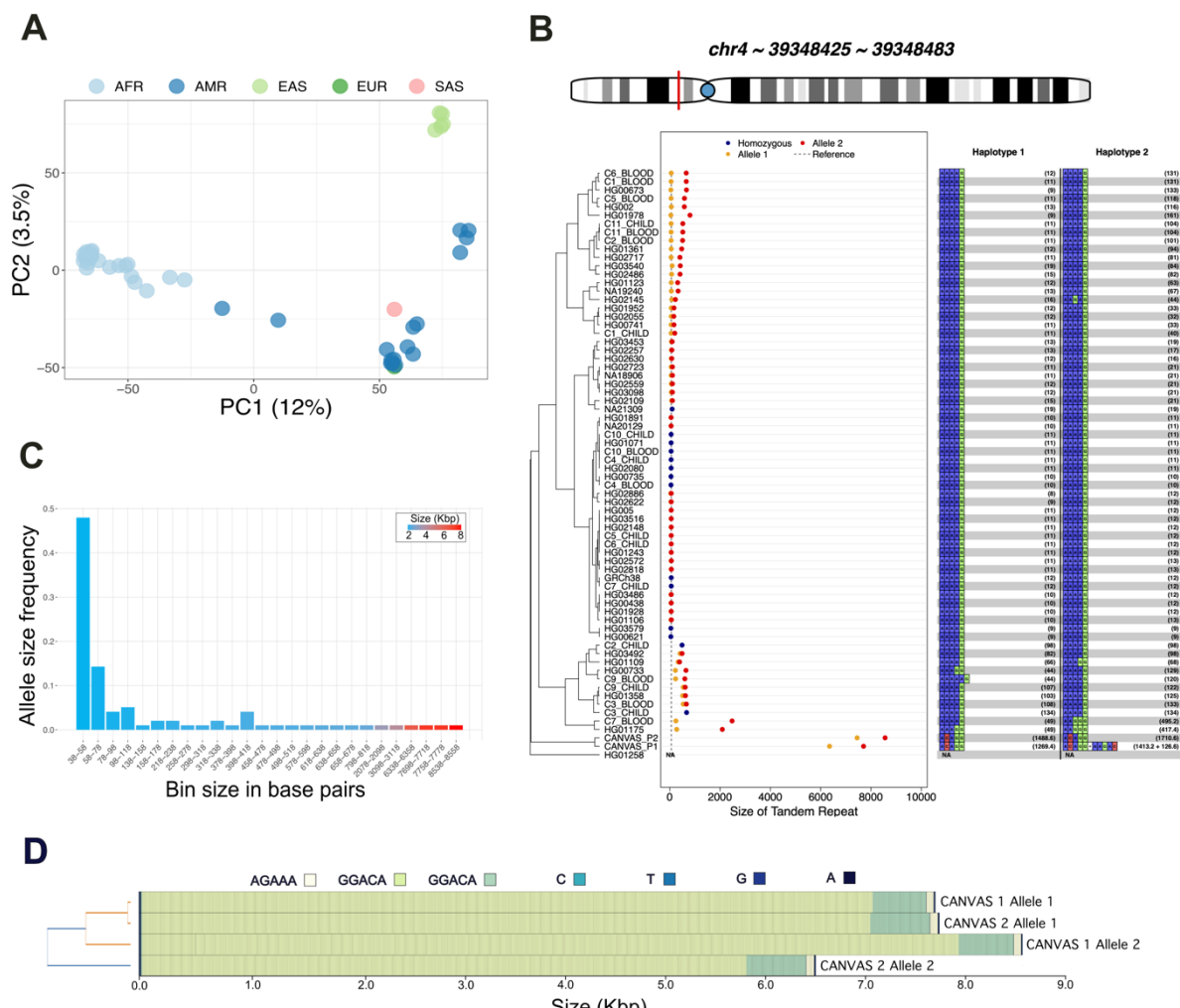
223 **2.3 TREAT's unified workflow enables diverse characterisations**
 224 **of tandem repeats**

225 We applied TREAT's unified workflow to characterise TRs in a population and clinical setting.
 226 First, we genotyped the set of 161K TRs in 47 genomes from the Human Pangenome

227 Research Consortium (HPRC),³⁴ for which PacBio HiFi data was available. We then extracted
228 the top 20% most variable TRs (N=32,208, based on the coefficient of variation, see *Methods*),
229 and performed a principal component analysis (PCA, *Figure 3A*) on the joint allele sizes (*i.e.*
230 the sum of the maternal and paternal alleles). We found that PC1 explained 12% of the total
231 variance and genetically represented the African-American axis, while PC2 explained 3.5% of
232 variance and corresponded to the American-Asian axis. The explained variance was similar
233 to that of a PCA including 40/47 matching samples and 30,544 random common (minor allele
234 frequency >10%) Single Nucleotide Polymorphisms (SNPs) (PC1: 14%, PC2: 4%, *Figure S7*).
235
236 We then used TREAT's outlier analysis to detect and score extreme TR expansions or
237 contractions of 35 clinically relevant TRs (*Table S1*) in 47 genomes from the HPRC, as well
238 as two Dutch CANVAS patients and 10 parent-offspring duos (see *Methods*).^{35,36} The two
239 CANVAS patients were previously characterised to harbour expansions in the intronic TR in
240 *RFC1*.³⁵ For all individuals, PacBio HiFi data were generated with Sequel 2 instrument. In total,
241 we identified 30 instances where the TR length in certain samples were significantly different
242 from the distribution of TR lengths across all 69 genomes. The most significant deviations
243 were observed for the two CANVAS patients in the TR intronic of *RFC1* gene ($p<2\times10^{-16}$ for
244 both patients, *Figure 3B-D*). The joint allele size for these samples was 78- and 89-fold higher
245 than the median TR size across all 69 genomes. Significant TR expansions were also found
246 in the TR in *ATXN8* gene (HG01123 sample, $p<2\times10^{-16}$, *Figure S8*), and in *DMD* gene
247 (HG02622 sample, $p=6.90\times10^{-3}$, *Figure S9*). Interestingly, in the TR intronic of *RFC1* gene,
248 we also observed a significant heterozygous expansion in one parent of the parent-offspring
249 duos ($p=1.7\times10^{-3}$ and $p=5.18\times10^{-11}$, respectively for the short and long alleles, *Figure 3B*).
250 Unexpectedly, the child reported a homozygous non-expanded genotype, suggesting a mis-
251 assembly or an allele dropout.
252

253 Finally, we applied TREAT to characterise unique TRs that are present in CHM13 reference
254 genome but absent in GRCh38 across the 47 HPRC genomes. We first curated a set of ~864K
255 genome-wide TRs in the CHM13 reference genome (see *Methods*). We evaluated genotyping
256 accuracy by applying TREAT/*otter* to CHM13-aligned long-read datasets of HG002 (PacBio's
257 Revio and Sequel 2 as well as ONT's Duplex and Simplex). We observed similar
258 performances as those observed when using ~161K TRs from GRCh38 (see *Figure S10* and
259 *Supplementary Results*). These results showcase *otter* and TREAT's ability to *de novo*
260 characterise TRs across different reference genomes, and without prior knowledge of TR motif
261 composition. Based on a CHM13-to-GRCH38 liftover procedure, we found 1017 unique TRs
262 present in CHM13 and absent in GRCh38, 37% of which overlapped coding sequences
263 (*Supplementary Methods* and *Table S2*). We used TREAT/*otter* to characterise these TRs
264 across the 47 HPRC genomes and found a mean TR size of 129 bp (median=45 bp), mainly
265 composed of trinucleotide motifs (42%), followed by homopolymers (26%), and 6+ nucleotide
266 motifs (22%, *Figure S11*).

267



268 *Figure 3: TREAT visualisation and analysis modules. A. The PCA of the ancestry-based analysis based*
 269 *on the 20% most variable TRs across 47 HPRC genomes. B. The main TR in the RFC1 gene. Y-axis:*
 270 *individuals, X-axis: TR size (in bp). Blue dots: smaller allele, orange dots: larger allele, red dots;*
 271 *homozygous genotypes. Dashed line: the allele in the reference genome GRCh38. The right side of the*
 272 *plot reports, for each sample and each allele, the motif and relative number of copies. The TR length of*
 273 *the two CANVAS patients were identified as significant outliers compared to the length-distribution of*
 274 *47 samples from the HPRC. C. The distribution of allele sizes for the TR in RFC1 gene. D. Motif*
 275 *representation in CANVAS patients, as produced with MotifScope.³⁷*
 276
 277

278 2.4 Tandem repeats may be sensitive to coverage dropouts in
279 long-read sequencing

280 A closer investigation of PacBio long-read data revealed unexpected drops of coverage in
281 clinical TRs, consequently leading to mis-genotyping of disease-associated TRs. One
282 example is the CANVAS-associated intronic TR in *RFC1*, where the most common allele
283 consists of an (AAAAG)11 motif, with a total size of ~55bp. In CANVAS patients, the TR can
284 range from 2-10 Kbp in total length (*Figure 3B-D and Supplementary Results*). In one parent-
285 child duo, we found that the parent harboured an expanded heterozygous version of the TR:
286 a shorter allele with a total length of 244 bp with the (AAAAG)50 motif; and a longer allele with
287 a total length of 2.49 Kbp, composed primarily of the (AAGGG)490 motifs (*Figure 4A*). Long-
288 read sequencing of brain tissue from the same individual (PacBio Sequel 2) confirmed these
289 results, although the longer allele was further expanded by 180 bp (36 additional motif-copies),
290 suggesting a somatic expansion in the brain relative to blood (*Figure 4A*). However, long-read
291 data from the child yielded a homozygous allele-sequence of 63 bp with the (AAAAG)12 motif
292 (*Figure 4A*). This was unexpected as at least one of the two allele-sequences from the parent
293 should be inherited in the child. A closer analysis of HiFi long-read-pileup overwhelmingly
294 supported this genotype. However, we observed an abnormal coverage drop in both the
295 parent and child for this TR, which was alleviated when including non-HiFi data
296 (*Supplementary Results*). After merging HiFi and non-HiFi data of the child, TREAT/otter
297 correctly assembled the expanded allele-sequence at 2.65 Kbp in size with (AAGGG)>374.
298 Penta-repeat primed PCR (RP-PCR) confirmed that both parent and child harboured repeat
299 expansions separately composed of the (AAAAG) and (AAGGG) motifs (*Figure S12*).
300 Therefore, HiFi data alone failed to capture this expanded allele-sequence, which was
301 recoverable when including the non-HiFi data.

302

303 We observed similar situations of abnormal coverage drops in PacBio data in a separate
304 intronic TR in *ABCA7*, previously associated with Alzheimer's disease (AD). We
305 experimentally validated the lengths of this TR using Southern Blotting in a subset of nine
306 centenarians for which long-read sequencing was performed (*Figure S13 and Supplementary*
307 *Methods*). The local HiFi coverage for these individuals ranged 1-7x (*Figure 4B* and
308 *Supplementary Results*). The correlation between experimentally validated alleles and HiFi-
309 based alleles was 0.58 (Pearson correlation, *Figure 4B*). However, the inclusion of non-HiFi
310 data increased read-support by four-fold to an average coverage of 22x. As a result, the
311 correlation with experimentally validated allele sizes increased to 0.99 (*Figure 4B*). These
312 results highlight standing challenges of characterising TRs with long-read sequencing data,
313 and suggest systematic biases of long-read sequencing in certain genomic regions.

314
315 The above observations motivated us to systematically characterise genome-wide coverage
316 drops of TRs across long-read sequencing technologies. We did this by investigating coverage
317 drops in the curated set of ~864K genome-wide TRs in the CHM13 reference genome, using
318 both PacBio and ONT long-read datasets of HG002 at ~38x coverage (see *Supplemental*
319 *Results and Methods*). The average TR-length in this curated set was 93 bp, with motifs being
320 mostly 16+bp motifs (23%), followed by dinucleotide (18%), tetranucleotide (14%), and
321 homopolymers (13%, *Figure S4*). For each TR, we defined the *coverage ratio* by dividing the
322 local TR coverage vs. global genome-wide coverage. We found the average *coverage ratio* to
323 be 1.01, 1.02, 0.99 and 1.03, respectively for Sequel 2, Revio, ONT Simplex and Duplex
324 technologies. This indicated generally no unexpected coverage-drops in TRs (*Figure S14A*).
325 However, 486 (0.06%) unique TRs had ratios below 0.25 (*i.e.* a four-fold lower coverage than
326 expected based on the global average coverage), of which 454 (93%) were present in the
327 HG002 T2T reference assembly (*Table S3*). The majority of the low-coverage TRs (294/454,
328 65%) overlapped gene annotations, potentially leading to mis-genotyping that may impact
329 biological interpretation. Furthermore, we observed that some of these TRs were within 5 Kbp

330 of each other, suggesting that coverage drops can extend across multi-Kbp regions. Overall,
331 we observe significantly more low-coverage TRs in PacBio datasets compared to ONT
332 (OR=9.4, p-value<2x10-16, Fisher's exact test), with N=437 TRs (89%) being specific to
333 PacBio datasets. Moreover, 22% of these TRs (N=98) had low coverage in both Sequel 2 and
334 Revio datasets, suggesting potential systematic challenges in both technologies (*Figure*
335 *S14B-G*). This included the intronic TR in *ABCA7*, previously associated with Alzheimer's
336 disease. Interestingly, the average number of non-HiFi reads in these TRs was 10, indicating
337 that although reads were generated for these TRs, most were flagged as low-quality during
338 HiFi data generation.

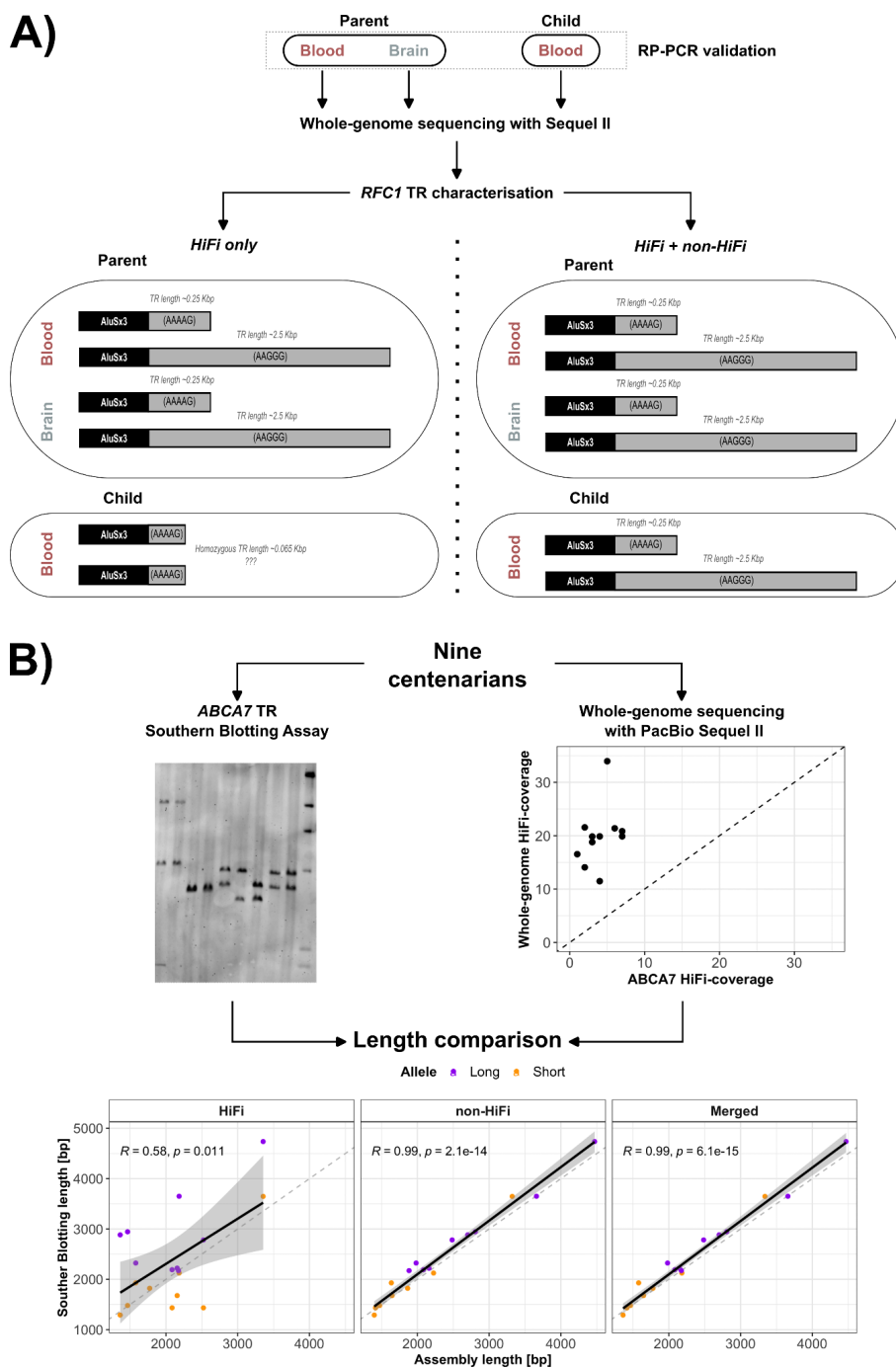
339

340 Within the ONT datasets, we observe significantly more low-coverage TRs in the Duplex
341 dataset relative to the Simplex dataset (OR=2.6, p-value=1.76x10-3, Fisher's exact test).

342

343 We characterised the sequences of all low-coverage TRs to investigate potential characteristic
344 features. When comparing the 454 low-coverage TRs with the remaining of ~864K genome-
345 wide TRs, we found that low-coverage TRs were longer (p-value = 8.68e-14; 493 bp longer
346 on average) and harboured higher GC-content (p-value = 2.28e-50; 17.4% higher on
347 average). A comparison of dinucleotide content revealed that AG, CC, CG, CT, and GG
348 dinucleotides were significantly enriched in the low-coverage TRs (*Figure S14H-I*). Moreover,
349 we found that G-quadruplex DNA secondary structures (G4s) were more likely to occur in low-
350 coverage TRs (p-value=2.48e-45; 3.76% higher, *Figure S14H* and *Supplementary Methods*).

351



360 available. When adding non-HiFi data, we could recover the expanded alleles in the child that were
361 missed by HiFi data alone.

362

363 **2.5 Comparing tandem repeats across multiple genomes in a
364 case-control setting**

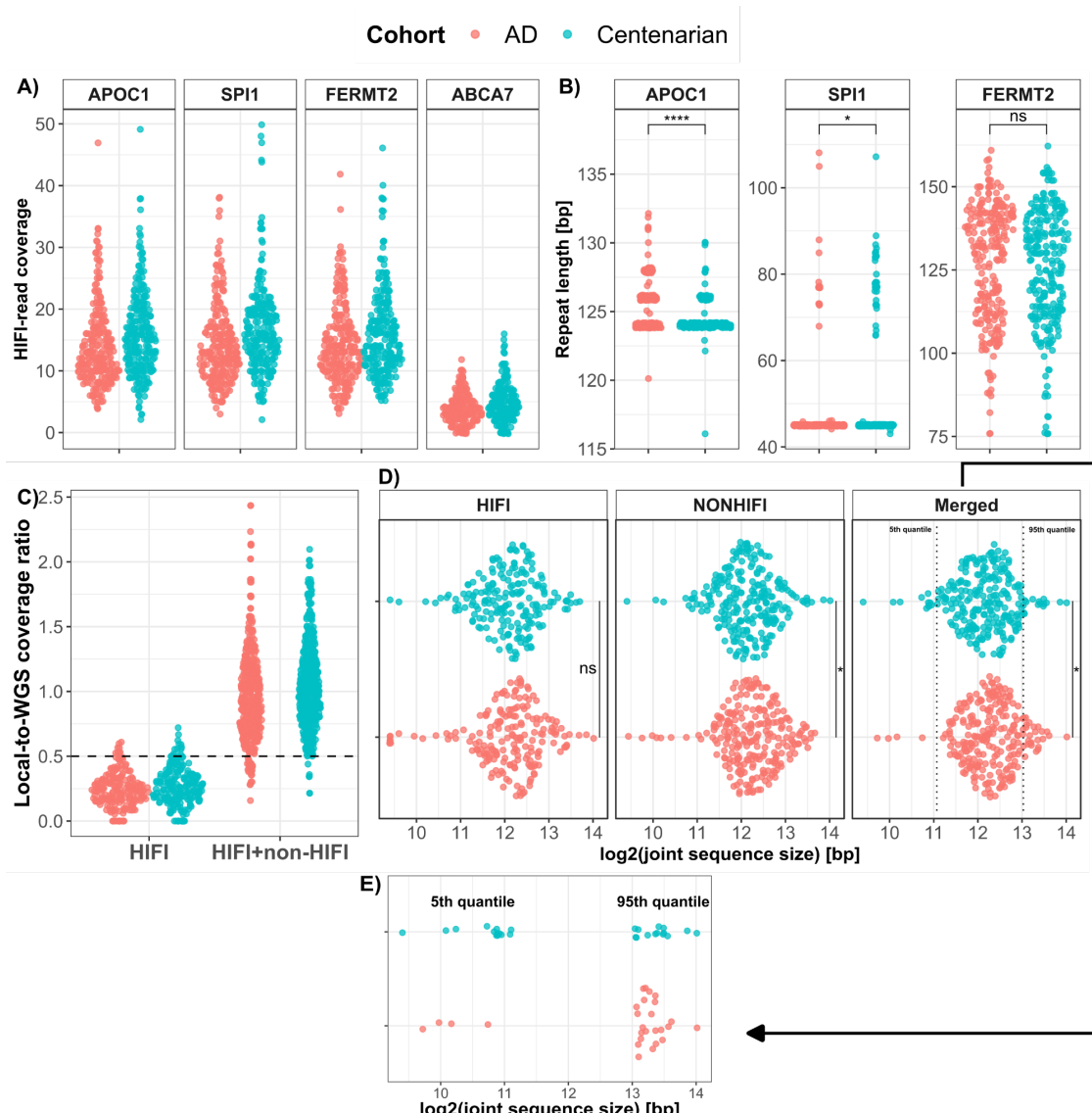
365 With the acquired knowledge about possible allele dropouts in TRs, we used TREAT/otter in
366 a case-control setting to replicate the association of four TRs that were previously shown to
367 associate with Alzheimer's Disease (AD) risk (*Table 1, Table S4*). We did so by using a set of
368 246 AD patients (mean age = 67.9±9.8, 70% females) and N=248 cognitively healthy
369 centenarians (mean age = 101.2±2.5, 70% females) that were sequenced with PacBio Sequel
370 2 instrument (*Methods and Figure S15*).³⁶ Across all 494 genomes, we observed a median
371 coverage (HiFi data) of 14, 15, 14, and 4, respectively for the TRs in *APOC1*, *SPI1*, *FERMT2*,
372 and *ABCA7* (*Figure 5A*). The combined allele size (*i.e.* the sum of the maternal and paternal
373 alleles) of the TR nearby *APOC1* (chr19:44921096-44921134) was significantly expanded in
374 AD patients compared to cognitively healthy centenarians ($\beta=0.38$, $p=2.63\times 10^{-9}$, *Figure*
375 *5B* and *Table 1*). In contrast, the short allele of the TR within *SPI1* gene was significantly
376 contracted in AD patients compared to cognitively healthy centenarians ($\beta=-0.03$,
377 $p=6.5\times 10^{-3}$, *Figure 5B* and *Table 1*). The direction of effect of these TRs was in line with the
378 original studies.^{38,39} We could not replicate the association of the TR within *FERMT2*
379 ($\beta=0.01$, $p=0.27$, short allele) (*Figure 5B* and *Table 1*).

380

381 For the intronic TR in *ABCA7*, we found significant expansions in AD cases after integrating
382 non-HiFi data ($\beta=8.63\times 10^{-5}$, $p=0.04$, joint allele size, *Figure 5C-D*). We note that 22
383 samples were omitted due to reduced coverage levels even after integrating HiFi and non-HiFi
384 data. We then identified TR size boundaries in the centenarian controls corresponding to the
385 5th and 95th percentiles of the joint TR allele sizes (2.2 Kbp and 8.4 Kbp, respectively). The

386 number of centenarians with a TR size lower than the 5th percentile was three-fold higher than
387 that of AD cases (1-tailed Fisher's exact test $p=0.023$, OR=3.2, *Figure 5E*), and the number of
388 AD cases with a TR size larger than the 95th percentile was two-fold higher than that of
389 centenarians (1-tailed Fisher's exact test $p=0.04$, OR=2.0, *Figure 5E*). Given the difficulties in
390 correctly assessing the allele sequences of this TR, we cannot exclude that additional samples
391 suffer from allelic dropouts, especially for the larger expanded allele-sequences.

392



393
394 *Figure 5: Replication of the association with AD of TRs in APOC1, SPI1, FERMT2 and ABCA7. A. The*
395 *coverage distribution of the four TRs in AD patients and cognitively healthy centenarians. B. The TR*
396 *size difference between AD patients and cognitively healthy centenarians in APOC1, SPI1 and*
397 *FERMT2. For the associations, we used logistic regression models using the TR size as predictor for*

398 *AD case-control status. C. HiFi and combined HiFi + non-HiFi coverage distribution of the TR intronic*
399 *of ABCA7 gene. D. Comparison of the joint allele size of ABCA7 TR between AD cases and cognitively*
400 *healthy centenarians, respectively using HiFi data, non-HiFi data, and the merged dataset of HiFi and*
401 *non-HiFi. E. Number of AD cases and cognitively healthy centenarians in the lower 5th quantile and*
402 *upper 95th quantile. Quantiles were defined based on the distribution of the joint TR-allele size in the*
403 *centenarians. We tested for the differential enrichment of AD and centenarians in each quantile with*
404 *Fisher's exact tests.*

405

406 *Table 1: Replication of TR previously associated with Alzheimer's Disease (AD)*

	TRs previously associated with AD			
Region	chr19:44921096-44921134	chr11:47775208-47775243	chr19:1049436-1050066	chr14:52832909-52832938
Gene	APOC1	SPI1	ABCA7	FERMT2
Best model	Joint alleles	Short alleles	Joint alleles	Short alleles
Beta (OR)	0.38 (1.46)	-0.03 (0.97)	8.63x10-5 (1.01)	0.01 (1.01)
P-value	2.6x10-9	6.5x10-3	0.041	0.27
Original study	38014121	37745545	29589097	37745545
Original OR	NA	-0.01 (0.99)	4.5	0.01 (1.01)
Original model	Longer allele	Joint alleles	Individuals with alleles >5720 bp	Joint alleles
Original method	Logistic regression	Mixed linear models	Fisher's exact	Mixed linear models
Original p-value	4.3x10-10	NA	0.008	NA
Original samples	1489 AD vs. 1492 controls	6328 AD vs. 6580 controls	275 AD vs. 177 controls	6328 AD vs. 6580 controls
Data type	Short read sequencing	Short read sequencing	Southern blot	Short read sequencing

407 *Region: genomic coordinates of the TR with respect to GRCh38; Gene: the closest gene as reported in*
408 *the original publications; Best model: model that yielded the most significant association, in our*
409 *comparison: Short allele, Long allele or Joint alleles size; Beta (OR): effect size and relative Odds Ratio*
410 *with respect to AD: an increased TR size leads to increased AD risk for positive estimates; P-value: p-*
411 *value of association. We used logistic regression models using TR size (short allele, long allele and*
412 *combined allele size) as predictor for AD case-control status, using 246 AD patients (cases) and 248*
413 *cognitively healthy centenarians (controls); Original study: the Pubmed ID of the original study; Original*
414 *OR: the odds ratio as reported in the original study; Original model: model used for association in the*
415 *original study; Original method: method used for association in the original study; Original p-value: the*

416 *p-value reported in the original study; Original samples: the number of AD cases and controls used in*
417 *the original study; Data type: the data on which the association were identified.*

418 3. Discussion

419 In this study, we provide novel contributions to better characterise tandem repeats (TRs) with
420 long-read sequencing data. First, we present our novel tools, *otter* and TREAT, that provide a
421 unified workflow to accurately characterise TRs using both Pacific Bioscience (PacBio) and
422 Oxford Nanopore Sequencing Technologies (ONT) datasets. This enabled us to characterise
423 genome-wide TRs in patients with neurodegenerative diseases and genomes from the Human
424 Pangenome Research Consortium (HPRC). Second, we show that in rare instances, long-
425 read sequencing technologies can suffer from abnormal coverage drops in TRs due to
426 potential systematic challenges, particularly in PacBio's HiFi technology. These coverage
427 drops can lead to TR mis-genotyping, as we observed in CANVAS and Alzheimer's disease
428 (AD)-associated TRs. Finally, we applied TREAT/*otter* to a case-control setting and replicated
429 TRs previously associated with AD across 494 long-read sequenced AD patients and
430 cognitively healthy centenarian genomes.

431

432 Our benchmark of *otter* and TREAT highlighted state-of-the-art performances of our tools in
433 terms of TR genotyping and motif identification accuracy. We showed that *otter*, TREAT, and
434 other existing tools provide generally accurate characterisations of TRs on both PacBio and
435 ONT datasets, and with improved accuracies at higher sequencing coverages. Across
436 technologies, our benchmark revealed that PacBio leads to generally more accurate
437 genotypes for relatively smaller TRs, with PacBio and ONT having similar performances for
438 TRs ranging 500-1000 bp, and ONT leading to more accurate genotypes for larger TRs. These
439 results remained when using other distance metrics as well as in a similar benchmark using
440 the CHM13 reference genome and a larger set of genome-wide TRs.

441

442 Our systematic analysis of coverage drops revealed that overall, coverage drops of TRs are
443 rare (0.6%), and do not impact the overall genotyping performances of TREAT/*otter* and other
444 tools. However, our analysis relied on HG002, a highly homozygous genome sequenced at

445 high coverage (38x). Hence, TR coverage drops may be more prevalent in other (low-
446 coverage) genomes that harbour expanded TR sequences, especially those with GC-rich
447 sequences. TRs with coverage drops were often large (>500 bp), high in GC-content, and with
448 higher densities of predicted G-quadruplex DNA secondary structures (G4s). G4s have been
449 previously reported to reduce polymerase efficiency.⁴⁰ As PacBio's HiFi technology relies on
450 multiple successful passes of a DNA polymerase in a circular DNA template,²⁰ we speculate
451 that the interference of G4s might reduce the number of passes in the circular template,
452 possibly leading to lower quality reads (non-HiFi reads). Altogether, incidents of TR coverage
453 drops were enriched in PacBio's Revio and Sequel 2 datasets, and to a lower extent in ONT's
454 Duplex and Simplex datasets, with ONT Simplex suffering the least. Although rare, we showed
455 and experimentally validated that coverage drops in TRs can occur at clinically relevant TRs,
456 requiring extra attention when characterising these TRs. To this end, we showed that local vs.
457 global coverage ratio is an effective way to identify such problematic regions, and that for
458 PacBio, these regions can be (in part) rescued by adding noisier non-HiFi data, as shown for
459 the TRs in *ABCA7* and *RFC1* genes.

460
461 TREAT and *otter* can be used to genotype and characterise potentially any type of repetitive
462 sequences. However, this remains challenging for very large TRs spanning several kilobases,
463 for example those in telomeric and centromeric regions of the genome. We also note that
464 regions where sequencing error-rates exceed inter-allele dissimilarities may still be difficult to
465 genotype. As the error rate in ONT Simplex data is relatively higher than PacBio and ONT
466 Duplex, this is likely driving the lower genotyping accuracy observed in ONT Simplex. These
467 limitations are not only specific to TREAT and *otter*, but extend to other existing tools. With
468 newer sequencing technologies bringing longer read lengths (e.g., ONT ultra-long reads),
469 together with more complete reference genome assemblies, it might become possible to
470 genotype any satellite region (micro-, mini-, and macro-satellites) in the genome with TREAT
471 and *otter*.

472

473 We were able to replicate previously reported TRs associated with AD by comparing a cohort
474 of AD patients and cognitively healthy centenarians. We acknowledge that these TRs were
475 previously identified using different experimental methods (e.g. short-read sequencing,
476 southern blotting), and analyses strategies (logistic regressions, linear mixed models, fisher's
477 exact test).^{12,38,39} While this heterogeneity hampers the direct comparison of the effect size
478 estimates, all associations we observed were in the same direction as the original studies. In
479 particular, the TR intronic of *ABCA7* was shown to carry an odds ratio for AD of 4.5 when one
480 allele was expanded >5.7 Kbp.¹² Similarly, we observed that individuals carrying larger allele-
481 sequences were significantly associated with AD. However, in our cohort, the effect was
482 mainly driven by cognitively healthy centenarians having a shorter joint-allele size (i.e. more
483 AD-protection), rather than AD cases having a more expanded TR-sizes. While we cannot
484 exclude that we have missed some expanded genotypes due to allele dropouts, the
485 centenarians that we included were previously shown to be enriched with the protective alleles
486 in the majority of Single Nucleotide Polymorphisms (SNPs) associated with AD.⁴¹

487

488 In summary, *otter* and TREAT are flexible and accurate bioinformatics tools compatible with
489 different sequencing platforms and requiring minimal input requirements, that enable end-to-
490 end analysis and comparisons of tandem repeats in human genomes with broad applications
491 in research and clinical fields.

492 4. Methods

493 4.1 TREAT

494 The main analysis is the *assembly* analysis, which uses *otter* for TR genotyping, and is
495 followed by TR content characterisation (identification of motif and number of copies) on the

496 individual TR alleles. In addition to the *assembly* analysis, TREAT implements a *reads*
497 analysis. Here, TR genotyping is performed using an iterative clustering framework based on
498 TR sizes (*Supplementary Methods*). This is followed by TR content characterisation, which is
499 done on all individual reads (*Supplementary Methods* and *Supplementary Results*). This
500 analysis may be preferred when information from all reads is needed, for example for
501 performing a multiple sequence alignment, or when studying somatic instability.
502 In all cases, TR content characterisation is performed with *pytrf* (<https://github.com/lmdu/pytrf>).
503 When multiple motif annotations for the same sequence are found by *pytrf*, a consensus
504 representation of the repeat content is generated. Briefly, if the fraction of sequence annotated
505 with a given motif is >95%, then the relative motif is regarded as the best motif describing the
506 TR. In case two or more motifs are found, each describing a portion of the sequence, then the
507 intersection is calculated by intersecting the motif-specific start and end positions. If the
508 intersection is <90%, then the motifs and the relative number of copies are combined. For
509 example, for sequence TGTGTGTGTGTGTGGAGAGAGAGAGAGA, *pytrf* identifies (i) 7
510 copies of TG (ranging positions 1-14, 50% of the sequence covered), and (ii) 7 copies of GA
511 (ranging positions 15-28, 50% of the sequence covered). In this case, the combined sequence
512 annotation will be TG+GA, repeated 7+7 times (see *Supplementary Methods*).
513 TREAT's analysis module consists of an outlier-detection framework, and a case-control
514 analysis. The outlier-detection scores extreme variations in TR allele sizes across a set of
515 samples. Outliers are detected using a normalised distance that quantifies how far each allele
516 size is from the median allele size, scaled by the variability of the data (*Supplementary*
517 *Methods*). A p-value for each individual is then calculated by comparing each data point's
518 distance to a chi-squared distribution. The case-control analysis employs logistic regression
519 models to compare allele sizes (short allele, long allele, and joint allele size) between cases
520 and controls.

521 4.2 *Otter*: a stand-alone, fast, local assembler

522 *Otter* is a generic stand-alone method for generating fast local assemblies of a given region
523 or genotyping whole-genome *de novo* assemblies. *Otter* is the main genotyping engine of
524 TREAT assembly analysis. Briefly, given a region of interest, *otter* uses the `htslib` library to
525 identify spanning reads (region of interest is fully contained in the reads) and non-spanning
526 reads (only partially contained) in a given BAM file, and extracts the corresponding
527 subsequence per read based on their alignment (*Figure 1B*).⁴² When a reference genome is
528 provided, it will perform local read-realignments on non-spanning reads if it detects a clipping-
529 signal, which can indicate suboptimal mappings to due highly divergent sequences (*Figure*
530 *1B*). This is done by aligning (using WFA2-lib alignment library)⁴³ the flanking sequences of a
531 region (100 bp by default, modifiable with ‘--flank-size’ parameter) derived from the reference
532 genome onto each read, which are then used to recalibrate the corresponding subsequence
533 of the region of interest. Recalibrated non-spanning reads are reclassified as *spanning* if both
534 flanking sequences are successfully aligned with a minimum length and sequence similarity
535 (by default, 90% sequence similarity, modifiable with ‘--min-sim’ parameter). In the context of
536 TRs, this realignment procedure often correctly recalibrates the alignments of TRs with major
537 length and/or motif-composition differences relative to a reference genome.

538

539 *Otter* identifies unique allele-sequences by clustering spanning-reads via pairwise-sequence
540 alignment (*Figure 1B* and *Supplementary Methods*). To manage high somatic variation and/or
541 sequencing errors, *otter* estimates local baseline error-rates per region using a gaussian-
542 kernel density estimator. This produces a one-dimensional distribution of spanning pairwise-
543 sequence distances. In single homozygous allele-sequences, the distribution is unimodal
544 centred at 0. With multiple allele-sequences, the distribution is multimodal, where peaks
545 represent sequence errors between reads from different allele-sequences. *Otter* identifies
546 these peaks and performs hierarchical clustering, stopping when distances exceed the
547 densest peak, partitioning reads into initial clusters. This procedure is followed by a curation

548 step to ensure sufficient read support, adapting to local coverage (*Figure 1B*). If no maximum
549 number of alleles (α) is enforced, *otter* outputs all clusters. Otherwise, clusters below the
550 coverage threshold are merged, and if clusters exceed α , hierarchical clustering continues
551 until α clusters remain. *Otter* then generates a final consensus sequence per cluster via
552 pseudo-partial order alignment procedure of spanning and non-spanning reads inspired from
553 *Ye and Ma, 2016*.⁴⁴

554

555 4.3 Genomes included for testing

556 *HPRC*: Publicly available PacBio long-read HiFi data of 47 individuals from the Human
557 Pangenome Reference Consortium (HPRC) were downloaded (*Data Accession*).³⁴ For the
558 well characterised HG002 genome,³² we also downloaded data generated with Oxford
559 Nanopore (ONT, Duplex and Simplex chemistries) and PacBio Revio technologies. Finally,
560 we generated long-read sequencing data for HG002 using the PacBio Sequel 2 instrument
561 across three SMRT cells, keeping both HiFi and non-HiFi data. ONT data was aligned to the
562 reference genomes (GRCh38 and CHM13) using minimap2 (2.21-r1071, specifying -x map-
563 ont).⁴⁵ PacBio data was aligned using pbmm2 (1.9.0, specifying –preset CCS and –preset
564 SUBREADS respectively for HiFi and non-HiFi data).²⁰

565

566 *100-plus Study cohort and Alzheimer Dementia Cohort*: For the replication of TRs previously
567 associated with Alzheimer's Disease (AD), we used HiFi sequencing (Sequel 2) data from the
568 blood DNA of N=246 patients with AD from the Amsterdam Dementia Cohort (ADC),^{36,46} and
569 N=248 cognitively healthy centenarians from the 100-plus Study cohort.^{36,47} Ten cognitively
570 healthy centenarians were sequenced as a trio, including the blood-derived DNA from the
571 centenarian, the brain-derived DNA from the centenarian and blood-derived DNA from a child
572 of the centenarian. The combined set of a centenarian and child is referred to as parent-child

573 duo throughout the manuscript. Sequencing data pre-processing was conducted as previously
574 described (*Supplementary Methods*).³⁶

575

576 *CANVAS patients*: We used the HiFi data (Sequel 2) of two patients diagnosed with CANVAS
577 (Cerebellar ataxia with neuropathy and vestibular areflexia syndrome), caused by a TR
578 expansion in *RFC1* gene.³⁵

579

580 4.4 Evaluating *otter* and TREAT performances

581 *Comparison with existing tools*: We compared TREAT/*otter* to TRGT and LongTR.^{22,31} For the
582 comparison, we used the HG002 genome and a set of 161,382 TRs from PacBio's repeat
583 catalogue (version 0.3.0, available at
584 <https://github.com/PacificBiosciences/trgt/tree/main/repeats>). We compared the tools'
585 genotyped alleles to the expected alleles from the T2T assembly of HG002. As metrics, we
586 used (i) normalised edit distance, (ii) raw edit distance, (iii) allele size correlation between the
587 observed and expected alleles, and (iv) fraction of perfectly genotyped alleles. In addition, we
588 evaluated motif identification accuracy, and computational resources.

589

590 *TREAT/otter applications*: We compared the performances of TREAT assembly and reads
591 analyses by correlating the estimated TR allele sizes with each other (*Supplementary*
592 *Results*). Then, we used TRs for a population stratification analysis: using the set of 161K
593 TRs, we selected the top 20% most variable TRs based on the coefficient of variation (ratio of
594 standard deviation to the mean TR joint allele size). Then we applied Principal Component
595 Analysis (PCA) based on the joint allele sizes. For 40/47 matching samples with Single
596 Nucleotide Polymorphisms (SNP) data from the 1000Genome project,⁴⁸ we also performed
597 PCA based on 30,544 randomly sampled common (minor allele frequency >10%) SNPs.

598 To evaluate clinical applicability, we applied the TREAT/otter outlier analysis module on the
599 combined dataset of 47 HPRC genomes plus the two CANVAS patients and the ten parent-
600 child duos. For this analysis, we focused on 35 clinically relevant TRs (*Table S1*), that were
601 previously associated with neurological diseases.^{7,8,12} Finally, TREAT/otter case-control
602 analysis module was used to replicate the association of four TRs that were previously
603 associated with Alzheimer's Disease (AD).^{12,38,39} The commands used for the outlier and case-
604 control analyses are available in *Supplementary Methods*.

605

606 4.5 Systematic analysis of allele dropouts in tandem repeats

607 *Curated set of TRs in CHM13*: We downloaded and curated repeat annotations for the CHM13
608 reference genome (version 2.0, <https://github.com/marbl/CHM13>, *Supplementary Methods*).
609 This curated dataset counted 864,424 TRs genome-wide. We extracted the corresponding
610 parental and maternal allele-sequences in HG002 for these TRs by aligning the HG002 T2T
611 assembly (version 0.7) to CHM13.³²

612

613 *TRs unique to CHM13*: We first genotyped the 864K TRs using *otter* in HG002 from different
614 technologies (Sequel 2, Revio, Simplex and Duplex), and at different coverage levels (5x, 10x,
615 15x, 20x, 25x and 30x), and calculated the normalised edit distance between observed and
616 expected TR alleles (*Supplementary Results*). We then focussed on a set of TRs present in
617 CHM13 and absent in GRCh38, and used TREAT/otter to characterise the repeat content of
618 these TRs in 47 genomes from HPRC.

619

620 *Evaluation of coverage drops in TR*: Using HG002 data from Sequel 2, Revio, Simplex and
621 Duplex technologies (~30x coverage each), we calculated the ratio between local TR
622 coverage and average global coverage. TRs where this ratio was <0.25 were regarded as low-
623 coverage TRs. We then investigated sequence characteristics of low-coverage TR, including

624 average size, dinucleotide content, and propensity to form G-quadruplex DNA secondary
625 structures (G4s). For the latter, we used pqsfinder (v2.10.1) with 'min_score = 20' parameter.⁴⁹
626

627 **Data access**

628 Human Pangenome Consortium data is publicly available and can be downloaded from
629 https://github.com/human-pangenomics/HPP_Year1_Data_Freeze_v1.0?tab=readme-ov-
630 [file](#).

631 Long-read sequencing data generated with PacBio Sequel 2 for the 2 CANVAS patients as
632 well as 246 AD patients and 248 cognitively healthy centenarians is available upon submission
633 of a research proposal to the Alzheimer Genetics Hub (AGH, <https://alzheimergenetics.org/>).

634

635 **Consent statement**

636 The Medical Ethics Committee of the Amsterdam UMC and Radboud UMC approved all
637 studies. All participants and/or their legal representatives provided written informed consent
638 for participation in clinical and genetic studies.

639

640 **Funding**

641 Part of the work in this manuscript was carried out on the Cartesius supercomputer, which is
642 embedded in the Dutch national e-infrastructure with the support of SURF Cooperative.
643 Computing hours were granted to H. H. by the Dutch Research Council (100plus: project#
644 vuh15226, 15318, 17232, and 2020.030; Role of VNTRs in AD; project# 2022.31, Alzheimers
645 Genetics Hub project# 2022.38). N.T is appointed at ABOARD and H.H, M.R, S.L are

646 recipients of ABOARD, a public-private partnership receiving funding from ZonMW
647 (#73305095007) and Health~Holland, Topsector Life Sciences & Health (PPP-allowance;
648 #LSHM20106).^{41,50} This work is supported by a VIDI grant from the Dutch Scientific Counsel
649 (#NWO 09150172010083) and a public-private partnership with TU Delft and PacBio,
650 receiving funding from ZonMW and Health~Holland, Topsector Life Sciences & Health (PPP-
651 allowance), and by Alzheimer Nederland WE.03-2018-07. S.L. is recipient of ZonMW funding
652 (#733050512). H.H. was supported by the Hans und Ilse Breuer Stiftung (2020), Dioraphte
653 16020404 (2014) and the HorstingStuit Foundation (2018). Acquisition of the PacBio Sequel
654 2 long read sequencing machine was supported by the ADORE Foundation (2022).
655

656 **Conflicts of interest**

657 All authors declare no conflict of interest.

658

659 **Acknowledgements**

660 We are grateful to all the reviewers involved in the peer-review process for their comments
661 which have largely improved our manuscript.

662

663 **References**

- 664 1. Hannan, A. J. Tandem repeats mediating genetic plasticity in health and disease. *Nat Rev
665 Genet* **19**, 286–298 (2018).
- 666 2. Lynch, M. *et al.* A genome-wide view of the spectrum of spontaneous mutations in yeast.
667 *Proc Natl Acad Sci U S A* **105**, 9272–9277 (2008).
- 668 3. Pearson, C. E., Edamura, K. N. & Cleary, J. D. Repeat instability: mechanisms of dynamic

669 mutations. *Nat Rev Genet* **6**, 729–742 (2005).

670 4. Subramanian, S., Mishra, R. K. & Singh, L. Genome-wide analysis of microsatellite
671 repeats in humans: their abundance and density in specific genomic regions. *Genome Biol*
672 **4**, R13 (2003).

673 5. Linthorst, J. *et al.* Extreme enrichment of VNTR-associated polymorphicity in human
674 subtelomeres: genes with most VNTRs are predominantly expressed in the brain. *Transl*
675 *Psychiatry* **10**, 369 (2020).

676 6. Dumbovic, G., Forcales, S.-V. & Perucho, M. Emerging roles of macrosatellite repeats in
677 genome organization and disease development. *Epigenetics* **12**, 515–526 (2017).

678 7. McMurray, C. T. Mechanisms of trinucleotide repeat instability during human
679 development. *Nat Rev Genet* **11**, 786–799 (2010).

680 8. Khristich, A. N. & Mirkin, S. M. On the wrong DNA track: Molecular mechanisms of repeat-
681 mediated genome instability. *J Biol Chem* **295**, 4134–4170 (2020).

682 9. Stevanovski, I. *et al.* Comprehensive genetic diagnosis of tandem repeat expansion
683 disorders with programmable targeted nanopore sequencing. *Sci Adv* **8**, eabm5386
684 (2022).

685 10. Yu, S. *et al.* Fragile X Genotype Characterized by an Unstable Region of DNA. *Science*
686 **252**, 1179–1181 (1991).

687 11. DeJesus-Hernandez, M. *et al.* Expanded GGGGCC hexanucleotide repeat in noncoding
688 region of C9ORF72 causes chromosome 9p-linked FTD and ALS. *Neuron* **72**, 245–256
689 (2011).

690 12. On Behalf of the BELNEU Consortium *et al.* An intronic VNTR affects splicing of ABCA7
691 and increases risk of Alzheimer's disease. *Acta Neuropathologica* **135**, 827–837 (2018).

692 13. De Roeck, A., Van Broeckhoven, C. & Sleegers, K. The role of ABCA7 in Alzheimer's
693 disease: evidence from genomics, transcriptomics and methylomics. *Acta Neuropathol*
694 **138**, 201–220 (2019).

695 14. Dolzhenko, E. *et al.* ExpansionHunter: a sequence-graph-based tool to analyze variation

696 in short tandem repeat regions. *Bioinformatics* **35**, 4754–4756 (2019).

697 15. Gymrek, M., Golan, D., Rosset, S. & Erlich, Y. lobSTR: A short tandem repeat profiler for
698 personal genomes. *Genome Res.* **22**, 1154–1162 (2012).

699 16. Kristmundsdóttir, S., Sigurpálsdóttir, B. D., Kehr, B. & Halldórsson, B. V. popSTR:
700 population-scale detection of STR variants. *Bioinformatics* **33**, 4041–4048 (2017).

701 17. Bakhtiari, M., Shleizer-Burko, S., Gymrek, M., Bansal, V. & Bafna, V. Targeted genotyping
702 of variable number tandem repeats with adVNTR. *Genome Res.* **28**, 1709–1719 (2018).

703 18. Gelfand, Y., Hernandez, Y., Loving, J. & Benson, G. VNTRseek-a computational tool to
704 detect tandem repeat variants in high-throughput sequencing data. *Nucleic Acids Res* **42**,
705 8884–8894 (2014).

706 19. Eslami Rasekh, M., Hernández, Y., Drinan, S. D., Fuxman Bass, J. I. & Benson, G.
707 Genome-wide characterization of human minisatellite VNTRs: population-specific alleles
708 and gene expression differences. *Nucleic Acids Research* **49**, 4308–4324 (2021).

709 20. Wenger, A. M. *et al.* Accurate circular consensus long-read sequencing improves variant
710 detection and assembly of a human genome. *Nat Biotechnol* **37**, 1155–1162 (2019).

711 21. Sereika, M. *et al.* Oxford Nanopore R10.4 long-read sequencing enables the generation
712 of near-finished bacterial genomes from pure cultures and metagenomes without short-
713 read or reference polishing. *Nat Methods* **19**, 823–826 (2022).

714 22. Dolzhenko, E. *et al.* Characterization and visualization of tandem repeats at genome scale.
715 *Nat Biotechnol* (2024) doi:10.1038/s41587-023-02057-3.

716 23. Chiu, R., Rajan-Babu, I.-S., Friedman, J. M. & Birol, I. Straglr: discovering and genotyping
717 tandem repeat expansions using whole genome long-read sequences. *Genome Biol* **22**,
718 224 (2021).

719 24. Masutani, B., Kawahara, R. & Morishita, S. Decomposing mosaic tandem repeats
720 accurately from long reads. *Bioinformatics* **39**, btad185 (2023).

721 25. Gustafson, J. A. *et al.* *Nanopore Sequencing of 1000 Genomes Project Samples to Build*

722 a Comprehensive Catalog of Human Genetic Variation.

723 <http://medrxiv.org/lookup/doi/10.1101/2024.03.05.24303792> (2024)

724 doi:10.1101/2024.03.05.24303792.

725 26. Ren, J., Gu, B. & Chaisson, M. J. P. vamos: variable-number tandem repeats annotation

726 using efficient motif sets. *Genome Biol* **24**, 175 (2023).

727 27. Gouil, Q. & Keniry, A. Latest techniques to study DNA methylation. *Essays in Biochemistry*

728 **63**, 639–648 (2019).

729 28. Liu, Y. *et al.* DNA methylation-calling tools for Oxford Nanopore sequencing: a survey and

730 human epigenome-wide evaluation. *Genome Biol* **22**, 295 (2021).

731 29. Amarasinghe, S. L. *et al.* Opportunities and challenges in long-read sequencing data

732 analysis. *Genome Biol* **21**, 30 (2020).

733 30. Mirkin, S. M. Expandable DNA repeats and human disease. *Nature* **447**, 932–940 (2007).

734 31. Ziae Jam, H. *et al.* LongTR: genome-wide profiling of genetic variation at tandem repeats

735 from long reads. *Genome Biol* **25**, 176 (2024).

736 32. Jarvis, E. D. *et al.* Semi-automated assembly of high-quality diploid human reference

737 genomes. *Nature* **611**, 519–531 (2022).

738 33. Baid, G. *et al.* DeepConsensus improves the accuracy of sequences with a gap-aware

739 sequence transformer. *Nat Biotechnol* (2022) doi:10.1038/s41587-022-01435-7.

740 34. Wang, T. *et al.* The Human Pangenome Project: a global resource to map genomic

741 diversity. *Nature* **604**, 437–446 (2022).

742 35. van de Pol, M. *et al.* Detection of the ACAGG Repeat Motif in RFC1 in Two Dutch Ataxia

743 Families. *Mov Disord* **38**, 1555–1556 (2023).

744 36. Salazar, A. *et al.* An *AluYb8* Retrotransposon Characterises a Risk Haplotype of

745 *TMEM106B* Associated in *Neurodegeneration*.

746 <http://medrxiv.org/lookup/doi/10.1101/2023.07.16.23292721> (2023)

747 doi:10.1101/2023.07.16.23292721.

748 37. Zhang, Y. *et al.* MotifScope: A Multi-Sample Motif Discovery and Visualization Tool for

749 Tandem Repeats. <http://biorxiv.org/lookup/doi/10.1101/2024.03.06.583591> (2024)

750 doi:10.1101/2024.03.06.583591.

751 38. Guo, M. H., Lee, W.-P., Vardarajan, B., Schellenberg, G. D. & Phillips-Cremins, J.
752 Polygenic burden of short tandem repeat expansions promote risk for Alzheimer's
753 disease. *medRxiv* 2023.11.16.23298623 (2023) doi:10.1101/2023.11.16.23298623.

754 39. Wang, H. *et al.* Structural Variation Detection and Association Analysis of Whole-Genome-
755 Sequence Data from 16,905 Alzheimer's Diseases Sequencing Project Subjects. *medRxiv*
756 2023.09.13.23295505 (2023) doi:10.1101/2023.09.13.23295505.

757 40. Lago, S. *et al.* Promoter G-quadruplexes and transcription factors cooperate to shape the
758 cell type-specific transcriptome. *Nat Commun* **12**, 3885 (2021).

759 41. Tesi, N. *et al.* Cognitively healthy centenarians are genetically protected against
760 Alzheimer's disease. *Alzheimer's & Dementia* **20**, 3864–3875 (2024).

761 42. Bonfield, J. K. *et al.* HTSlib: C library for reading/writing high-throughput sequencing data.
762 *Gigascience* **10**, giab007 (2021).

763 43. Marco-Sola, S. *et al.* Optimal gap-affine alignment in $O(s)$ space. *Bioinformatics* **39**,
764 btad074 (2023).

765 44. Ye, C. & Ma, Z. (Sam). Sparc: a sparsity-based consensus algorithm for long erroneous
766 sequencing reads. *PeerJ* **4**, e2016 (2016).

767 45. Li, H. Minimap2: pairwise alignment for nucleotide sequences. *Bioinformatics* **34**, 3094–
768 3100 (2018).

769 46. van der Flier, W. M. & Scheltens, P. Amsterdam Dementia Cohort: Performing Research
770 to Optimize Care. *Journal of Alzheimer's Disease* **62**, 1091–1111 (2018).

771 47. Holstege, H. *et al.* The 100-plus Study of cognitively healthy centenarians: rationale,
772 design and cohort description. *European Journal of Epidemiology* (2018)
773 doi:10.1007/s10654-018-0451-3.

774 48. 1000 Genomes Project Consortium *et al.* A global reference for human genetic variation.
775 *Nature* **526**, 68–74 (2015).

776 49. Hon, J., Martínek, T., Zendulka, J. & Lexa, M. pqsfinder: an exhaustive and imperfection-

777 tolerant search tool for potential quadruplex-forming sequences in R. *Bioinformatics* **33**,
778 3373–3379 (2017).

779 50. Dreves, M. A. E. *et al.* Rationale and design of the ABOARD project (A Personalized
780 Medicine Approach for Alzheimer’s Disease). *Alzheimers Dement (N Y)* **9**, e12401 (2023).

781